

Improving modeling of tides on the continental shelf off the west coast of India

L. Testut^{1,2} and A. S. Unnikrishnan²

¹Laboratoire d'Etudes en Géophysique et Océanographie Spatiales, 14 av. Edouard Belin, 31400
Toulouse, France

²CSIR- National Institute of Oceanography, Dona Paula, Goa, 403004, India

Additional Index Words: altimetry, tide constituents, tidal modeling, continental shelf, Gulf of Khambhat

Abstract

Global tidal solutions are sometimes inaccurate in coastal regions. This is particularly true in some regions of the northern Indian Ocean, which are characterized by wide continental shelves and large tidal ranges. We show that these global solutions are inaccurate on the shelf region off Mumbai, off the west coast of India. In this region, the shelf is very wide and it opens into the Gulf of Khambhat, where large tides are observed. Moreover, it is noticed that in regions of large semi-diurnal tides in the Bay of Bengal, such as, the head Bay, Gulf of Martaban etc., global tidal solutions are not accurate. In the present work, we focus on the shelf region off the west coast of India. We used a new approach in developing a high resolution hydrodynamic tidal model for the inner shelf region (8°N to 22°N). The open boundary of the model is aligned to the altimetric tracks, which allowed to prescribe boundary conditions obtained directly from observations. It is shown that the tidal solutions at the coast are much improved compared to those obtained from the global solutions and that on the wide shelf portion and the Gulf of Khambhat the improvement has been considerable.

INTRODUCTION

Since the availability of sea level data from altimetry, information on tides in the open ocean has improved considerably. There had been many studies on intercomparison among different tidal models (Andersen et al., 1995, Shum et al., 1997). In spite of the success of tidal models in the open ocean since the altimetric era, accurate prediction of tides in the coastal regions has been difficult using global models. Very near the coast, in the 0-15 km coastal band, altimetric data are not accurate and the use of satellite altimetry in those regions remains challenging (Vignudelliet al., 2011). New generation altimetry missions, such as the Indo-French Ka-band altimeter, SARAL/AltiKa, which is presently in orbit or the future wide swath altimeter Franco-US SWOT mission, will fly over coastal zones. These missions, based on new technologies, are expected to improve the spatial resolution and accuracy of sea surface elevations in the coastal band. In this perspective, accurate information on tides in coastal regions will become highly critical. At present, tidal information in many coastal waters around the globe are not provided with sufficient accuracy by the global tidal atlases. It has been shown by Fok *et al.* (2010) that their accuracies at the coast are region-dependent. Indeed, due to many factors, including their broad spatial resolution inadequate for many coastal regions, the tidal atlases presently used for generating sea-level anomaly fields from altimetric data, will not be able to provide sufficiently accurate corrections for the future altimetric missions in those shallow water regions. Large reduction in tidal correction can be expected from improvement of tidal models in shallow water regions and/or from the development of regional tidal models (Ray *et al.*, 2011). In addition to the problems near the coast, there are regions, for instance, the Coral Sea and Great Barrier Reef lagoon, Patagonian Shelf, where global tidal model results are found to be inaccurate due to complex topographical variations in the region. For example, Saraceno *et al.* (2009) showed the deficiency of global tidal models to accurately reproduce the tides on wide shelf of Patagonia. Burrage *et al.* (2003) developed a regional tidal model for the Great Barrier Reef lagoon and showed improvements in sea surface height anomalies derived using tidal corrections from the regional model. Another aspect of developing regional tidal models in coastal zone prone to cyclones is to improve the estimation of extreme water levels. Indeed the coastal flood risk uncertainty in the region appears to be very poorly integrated with tidal models (Lewis *et al.*; 2014).

So far, no studies have reported on the inaccuracies of global tidal solutions in coastal and shelf regions of the north Indian Ocean. Figure 1 shows the root mean square misfits (see methodology for definition) for the M2 constituent, between the solutions of two commonly used global tidal models, namely, GOT4.7 (Ray, 1999) and the latest hydrodynamic version, FES2012 (Carrère *et al.*, 2012). One can

notice that discrepancies are large in marginal seas such as Red Sea, Persian Gulf and Malacca Strait. Moreover, what is significant to note is that the largest discrepancies are found in regions such as the Gulf of Khambhat and the Gulf of Kutch along the west coast of India, head of the Bay of Bengal, Gulf of Martaban on the coast of Myanmar and off the southern coast of the eastern part of the Bay of Bengal. These regions are characterized by large semi-diurnal tides, where M2 amplitudes of about 1 m and larger (Unnikrishnan *et al.*, 1999; Murty and Henry, 1983; Sindhu and Unnikrishnan, 2013). These regions are largely dominated by the semi-diurnal tides and have usually large shelf width (about 200 km or more). Unnikrishnan (2010) reported amplification of semi-diurnal tides off the central west coast of India. In these regions, the error in M2 tidal correction reaches upto 15 cm, which is too large to derive accurate sea level anomalies from altimetric data.

In this paper, we propose a simple approach to improve the simulation of tides in coastal waters based on the opportunity given by the recent release of accurate along-track altimeter-derived tidal constants (Lyard *et al.*, 2009). In the present approach, we developed a 2D shallow-water finite element regional tidal model, whose open boundary is aligned along the altimetric track. The model was developed for the inner shelf region off the west coast of India. One of the characteristic features of this region is the widening of the shelf from south to north accompanied by a gradual northward increase in tidal range. Along the west coast of India, M2 is the largest tidal constituent with S2 and K1 having comparable amplitudes. Tidal range in the southern region of the coast, say, at Kochi, is of the order of 1 m, at Marmagao approximately at the central region of the coast, the maximum tidal range is about 2.2 m, while at Mumbai, tidal range reaches upto 5 m. The tidal regime of the shelf is mixed semi-diurnal type along the southern part of the coast (Kochi to Goa), which becomes more predominantly semi-diurnal towards north (Ratnagiri to Mumbai). Off Mumbai, large tidal ranges upto 3 m have been observed (Joseph *et al.*, 2009), based on measurements made from an oil-drilling platform at Mumbai High, located on the mid-shelf. The shelf in this region opens into the gulf of Khambhat, which is known for having one of the largest tidal ranges in the world. For instance, at Bhavnagar, a station located inside the Gulf, the maximum tidal range is more than 10 m. Presence of large tides inside the Gulf is attributed to the geometrical effects and quarter wave length resonance of semi diurnal tides (Nayak and Sheltie, 2003).

METHODS

We will present below the set-up of the model, the selected tide gauges observation and the validation methodology.

Model set-up

The hydrodynamic model used is the 2D barotropic shallow water module of the Toulouse *Unstructured* Grid Ocean model (T-UGOm) which is the follow up of MOG2D (Carrere and Lyard, 2003) for its time-stepping mode and of the FES tidal solution (Lyard *et al.*, 2006) for its spectral mode. The tidal equations are derived from the classical non-linear shallow water equations (Lynch and Gray, 1979). Assuming the existence of a dominant tidal constituent (in term of currents), the friction terms are given in a tensor form as a linear development of the non-linear bottom drag

$$\boldsymbol{\tau} = \frac{C_D}{H} \|\mathbf{u}\| \mathbf{u} \quad (1)$$

Where \mathbf{u} is the depth-averaged tidal velocity, H , the mean local depth and C_D a dimensionless friction coefficient (usually taken as 2.5×10^{-3}). Once the problem is fully linearized, the equations in complex form can be solved in the spectral domain. An iterative method is then used based on initialized approximate currents (about 1 m/s). Quasi-convergence is reached after a limited number of iterations, typically less than 10. Once the dominant constituent is resolved, the rest of the tidal spectrum can be solved in a one-step manner. The spectral and finite element characteristics of this model has proved to be the key factor of the success of the FES atlas at global scale (Le Provost *et al.*, 1994, Lyard *et al.*, 2006) as well as at regional scales (Maraldi *et al.*, 2007; Le Bars *et al.*, 2010; Testut *et al.*, 2012). The main advantage of the unstructured grid is that the spatial resolution can be increased in regions of interest (for example, near shelf break and at the coast), while keeping a reasonable number of mesh nodes in the domain. Because of its numerically low cost, the spectral mode also provides a very efficient way to test changing parameters such as bathymetry, friction, etc.

For the present work, we implemented a high resolution version of the T-UGOm model on the inner shelf along the western coast of India (Figure 2). The finite element mesh is composed of more than 15000 nodes with the mesh element size ranging from less than a 1 km at the coast to a maximum of 20 km in the middle of the shelf. The model domain is essentially located on the shelf region at depth less than 200 m. Based on a sensitivity analysis (see next section) we chose the improved bathymetric data (Sindhu *et al.*, 2007), which was developed by merging global bathymetry with information on

depths in shallow regions derived from the hydrographic charts published by the Indian Naval Hydrographic Office. The open boundary tidal conditions were taken from the new CTOH tidal constants product (<http://ctoh.legos.obs-mip.fr/products/coastal-products/coastal-products-1/tidal-constants>). This product contains along-track estimates of amplitude and phase lag for the major tidal constituents which are derived from the harmonic analysis of along-track observations from different altimetric missions (TOPEX/Poseidon, JASON 1&2). The open boundary conditions were prescribed using information at 319 points, extracted from altimetric track 66 and 79 (see Figure 2). The model was then forced with altimetric-derived elevation (amplitudes and phases) from 21 tidal constituents (M2, K2, S2, 2N2, MU2, N2, NU2, T2, K1, O1, OO1, P1, Q1, J1, M1, M4, MS4, MF, MM, MTM, SSA). The reference simulation is performed using a quadratic bottom friction ($C_D=1.6 \times 10^{-3}$) with the parameterization of the internal drag switch off.

Comparison with tide gauge data

The main database used for the validation purpose is the tidal harmonic constants (amplitude and phase) based on the Admiralty Tide Tables (ATT, 1996). Out of the 136 stations available in this database for the west coast of India, 66 fall inside the model domain. Among these 66 stations, only 39 were selected for the validation purposes (see Table 1 and Figure 2). The selection process was based on a multi-criteria analysis of each station regarding the length of the time series analyzed, consistency with neighboring stations as well as the distance between two neighboring stations. In order to keep independent of the validation process, the selection process did not involve any prior comparison with model. Some stations, such as Verem or Mangalore, which are located inside the estuaries, were discarded. Information in some stations was updated using recent measurements (P. Mehra, *personal communications*) and some more measurements (Joseph *et al.*, 2009, SanilKumar *et al.*, 2011) were used. The 39 selected stations are well distributed between 8°N and 21°N along the west coast of India and represent the variability of amplitude and phase observed along this coast (see Figure 2).

To provide a quantitative assessment of the model performance, the misfit RMS error (σ) for a single constituent at a single location is defined as the difference in the complex form (z) of the amplitude (A) and phase (G) obtained from the observation (shown with subscript obs) and the model (shown with subscript mod), as shown in equation (2). All phases in this study are referred to as Greenwich Meridian Time, GMT. A misfit gives at single location a quantitative estimate of the combined amplitude and phase difference between model and observation. The equation (3) gives the error associated with a

single site (σ_{site}) from the sum of the variance error of each constituent. The error associated with a given constituent ($\sigma_{constituent}$), as shown in equation (4), is given by the mean variance error over all different sites. Finally the Root Sum Square (hereafter RSS) is a combination of the misfits for all sites and all constituents following the equation (5). Then RSS gives a quantitative estimate of the accuracy of a model against an in situ dataset for a given number of constituents.

$$\sigma = \sqrt{\frac{1}{2} |\Delta z|^2} \quad ; \quad |\Delta z|^2 = |A_{obs} e^{i\phi_{obs}} - A_{mod} e^{i\phi_{mod}}| \quad (2)$$

$$\sigma_{site} = \sqrt{\frac{1}{2} \sum_{constituents} |\Delta z|^2} \quad (3)$$

$$\sigma_{constituent} = \sqrt{\frac{1}{2N_{site}} \sum_{site} |\Delta z|^2} \quad (4)$$

$$RSS = \sqrt{\frac{1}{2N_{site}} \sum_{site} \sum_{constituents} |\Delta z|^2} \quad (5)$$

The model performance was estimated based on the main 9 tidal constituents, namely, M2, S2, N2, K2, K1, O1, P1, Q1 and M4.

RESULTS

In order to evaluate the sensitivity of the model to important parameters, we performed a series of tests by varying: bathymetry, bottom friction and open boundary conditions. For each simulation, the complex RMS misfit (see equation 2) at each tide gauge location was computed. The sensitivity tests were performed using spectral runs of the model for the main semi-diurnal (M2) and diurnal (K1) constituents.

i) Sensitivity to Bathymetry

We ran the model with 8 different bathymetric data sets. Six of them were extracted from global grid (2 from the General Bathymetric Chart of the Oceans (GEBCO), 3 from the ETOPO dataset and the version 14.1 of the Smith and Sandwell (1997) bathymetry) and 2 of them from a regional modification of the ETOPO grid (Sindhu *et al.*, 2007). Below is the list and spatial resolution of used bathymetries.

- GEBCO_08 — a global 30 arc-second grid

- GEBCO One Minute Grid — a global one arc-minute grid (version 2009)
- ETOPO1 (Amante and Eakins (2009)) — a global one arc-minute grid
- ETOPO2v2 — a global two arc-minute grid
- ETOPO5 — a global five arc-minute grid
- Smith and Sandwell — a global one arc-minute grid
- SINDHU5 — modified ETOPO5
- SINDHU2 — modified ETOPO2

The results for this test are shown in Figure 3. Simulations using all the bathymetries give similar and fairly good results for the diurnal and semi-diurnal constituents in the southern part of the shelf (south of 17°N, of below Ratnagiri station no. 20). Indeed RMS error between model and observation for the M2 constituent is mostly around 2 cm for tidal amplitudes varying between 20 cm at Colachel to 70 cm at Ratnagiri, meaning that whatever may be the choice of the bathymetry, the model is within 10% error. Actually, most of the differences are observed in the region where the shelf is wide and inside the Gulf of Khambhat where the tidal amplitudes are large (> 70 cm for M2). For the semi-diurnal wave M2, simulations using the modified ETOPO are found to be the most accurate for this region (both 5 and 2 arc-minute version shows RMS misfit around 11 cm). Compared to all others bathymetries, the unmodified versions of ETOPO (5', 2' and 1') gave relatively poor results in the northern part of the shelf with up to 23 cm RMS error for ETOPO5. This gives an indication of the large improvement done by adding depth contours and soundings (Sindhu *et al.*, 2007). Interestingly, the GEBCO dataset provides slightly better solution for the 1 arc-minute compared to the 30 second-arc (around 12 cm RMS error). The simulation using Smith and Sandwell data gave similar result to that of the GEBCO series. For the diurnal wave, it is striking to note that the unmodified 2 arc-minute grid of ETOPO gives the best results with a wave RMS error below 6 cm while it is the second worst bathymetry for the semi-diurnal wave. The other bathymetric grids (except ETOPO5) give very consistent results for the K1 wave (between 6 and 7 cm RMS error). One can notice that in both semi-diurnal and diurnal case, the unmodified ETOPO5 shows large discrepancies for the Gulf of Khambhat, suggesting large errors of this version in the region.

ii) Sensitivity to Bottom friction

A series of simulations were carried out to tune the bottom friction coefficient over a large range of values. We used M2, the largest semi-diurnal constituent and K1, the largest diurnal constituent for further analysis (see Figure 4). As for bathymetry, the sensitivity to the bottom friction coefficient is greater for the northern part of the shelf, where it becomes wide. We found that in a numerical experiment, without any bottom friction, M2 wave is found to enter too rapidly into the Gulf of Khambhat. In this experiment, M2 arrives at station Umbargaon (no. 33) 2 hours in advance with a 12 cm amplitude decrease compared to observation. At the adjacent northern station, Bulsar (no. 34) the advance is by 2.6 h and amplitude decrease is 54 cm. The tide then reaches Hazira with 2.8 hours in advance and an amplitude decrease of 1.4 m. The correct M2 wave propagation is simulated by adding a small amount of bottom friction and the best comparison with observations for M2 is found for $C_D = 1.6 \times 10^{-3}$. This relatively low friction coefficient was found in regions of large sediment deposition, such as the Amazon estuary (Le Bars *et al.*, 2010). As shown in Figure 4, the M2 wave is very sensitive to change in C_D coefficient. For the K1 wave, the optimal friction coefficient is around 1×10^{-3} . As shown in Figure 4, the test without any friction gives good results for K1 and diurnal wave simulation degrades rapidly with increasing friction inside the Gulf of Khambhat.

iii) Sensitivity to Open Boundary Conditions

A series of tests were also performed using different open boundary conditions (OBC). The first experiment was done by forcing the model using tidal constituent (amplitude and phase) obtained from the CTOH altimeter product. Second, the model was forced at its open boundary with the output from the same 4 models that we used for validation (see next section and Figure 5). This test was performed using M2 and K1 only. As expected, GOT4.7 and TPXO7.2 give very similar results for K1 and M2. This is expected, as both these models assimilate altimetric data. However, using of OBC directly obtained from altimetry gives slightly better results for M2 than those obtained from GOT and TPXO atlases. For K1 results between GOT, TPXO and along-track constituent are very similar.

DISCUSSION

We used the classical approach to validate the regional model against the tide gauge dataset. For each of the 39 tide gauges (Figure 1, Table 1), eight major semi-diurnal and diurnal constituents (M2, S2, K2, N2, K1, O1, P1 and Q1) and the largest non-linear quarter-diurnal constituent (M4) were compared with those extracted from the model at the tide gauge locations. Figure 6 shows a comparison of the amplitude

and phase of the semi-diurnal wave M2 with those obtained from model. It can be seen that the amplitudes increase gradually northward, from about 0.2 m at the southernmost station, Colachel (station no. 1) to about 2 meters at Satpati (station no. 32), located at the entrance of the Gulf of Khambhat. The plot of phase distribution shows that M2 reaches a minimum, where the shelf starts to be wider at the latitude of Ratnagiri (station no. 20) and propagates northward and southward from this latitude. The model shows extremely good agreement with observations from Colachel (no. 1) to Bandra station (no. 29). Indeed, for this section (8°N-19°N), the model amplitudes mostly remain within 1 cm of accuracy with respect to the observations and the phase only by a few degrees (< 6 degrees). When the tide enters into the Gulf of Khambhat, amplitude rapidly increases and reaches to a maximum of about 3 m at Hazira (no. 35). The large amplification of the semi-diurnal constituents M2 and S2 can be seen on Figures 7 and 8. From Shrivardhan station, at the western entrance of the Gulf (18°N), where M2 is 80 cm and S2 is 40 cm to Hazira station, our northernmost station at 21.1 °N, the semi-diurnal signal is amplified by a factor of 2. The maximum semi-diurnal signal of the model is seen on the west side of the Gulf between Bulsar and Hazira. On the contrary, the diurnal constituent shows a small amplification between these two locations, with K1 (resp. O1) rising from 36.6 cm (resp. 17.9 cm) at Shrivardhan to 50.8 cm (resp. 23.3 cm) at Hazira. One can also notice from Figures 9 and 10 that the model slightly underestimates the diurnal signal inside the Gulf. From the entrance of the Gulf and inside the Gulf, the model starts to diverge from observations both in amplitude and phase (see Figures 7 to 10). Far inside the Gulf, north of Hazira, the model completely underestimates the tidal signal. Indeed, amplitudes greater than 3 m for M2 have been reported but very few observations are available to validate the model (Figure 7). Moreover, inside the Gulf, the bathymetry is highly variable due to changes in sediment deposition (Kunte, 2008) and bathymetry used in this very shallow water zone (see Figure 2) is probably not good enough to correctly model the tidal wave propagation. Table 1 summarizes the RMS misfits between the model simulation and the observations. The overall T-UGOm model RSS error is 12 cm.

Comparison of regional tidal model results with global models

In order to assess the improved performance of the regional model, we applied the same in situ validation using the main available global tidal atlases (GOT4.7, FES2004, FES2012, TPXO7.2). It is found that GOT4.7 is the best available global tidal solution for this region. The global hydrodynamic version of FES2012 does not improve global tidal solution in this region when compared to earlier version, despite the fact that it incorporated the improved bathymetry of Sindhu *et al.* (2007). FES2004 is suspected to

have assimilated tide gauges with phase errors in the west coast which could probably explain its low performance in the region. It can be noticed (Table 2) that significant improvement in the performance of the present regional model is found on the northern part of the shelf (from stations no. 21 to 39), where large tidal amplitudes occur (see Figures 7 and 8). The increase of resolution is most probably the main factor of improvement. Indeed the resolution in the Gulf of Khambhat is about one km in present model when compared to $\frac{1}{4}$ degree used in global tidal models (FES2004, GOT4.7, TPXO7.2). This resolution allows to better take into account the variability of the water depth in this shallow region. Then, due to the increase in mesh resolution, improved bathymetry, accurate boundary conditions and choice of appropriate bottom friction, the errors in the simulations of the regional model have been considerably reduced.

CONCLUSIONS

The present study illustrates the need for developing high-resolution regional tidal models for the north Indian Ocean, for providing accurate tidal corrections for processing altimetric data to generate sea-level anomalies. This becomes important in the context of current SARAL/Altika and future SWOT missions. One of the possible options is to use the altimetry tracks as an open boundary condition for developing regional models, which will permit to prescribe the boundary conditions from the tidal information derived from 20 years of altimetry. This approach was particularly useful in the present case where one of the track is parallel to the isobaths on a shelf, where strong amplification of semi-diurnal tides occurs. The present study shows that accuracy of tidal solutions can be considerably improved, even in a complex region such as the Gulf of Khambhat, where tides are very large. This implies that the variance of sea level anomaly (SLA), derived from this new tidal correction will be reduced by almost 60% in the region of the Gulf of Khambhat, when compared to the global solution (computed from Table 2). Moreover, the development of models, whose open boundary follows the altimetry tracks will facilitate merging of regional solutions into global tidal solutions.

Acknowledgments. This research was supported by the French National Space Agency (CNES) in the frame of the European Organization for the Exploitation of Meteorological Satellites (EUMETSAT) and CNES joint Ocean Surface Topography Science Team (OST-ST) Project. Altimetry data used in this study were developed, validated, and distributed by the CTOH/LEGOS, France. The authors thank Prakash Mehra for providing tidal constituents from recent measurements of NIO.

Literature Cited

- Admiralty Tide Tables, 1996. Hydrographer of the Navy Vol. 2, U.K.
- Andersen, O.B., Woodworth, P.L., and Flather, R.A., 1995. Intercomparison of recent ocean tide models. *Journal of Geophysical Research*, 100(C12), 25261-25282.
- Amante, C. and Eakins, B. W., 2009. ETOPO11 Arc-Minute Global Relief Model: Procedures, Data Sources and Analysis. *NOAA Technical Memorandum NESDIS NGDC-24*, 19 pp
- Burrage, D.M.; Steinberg, C.R.; Mason, L.B., and Bode, L., 2003. Tidal corrections for TOPEX altimetry in the Coral Sea and Great Barrier Reef Lagoon: Comparisons with long-term tide gauge records. *Journal of Geophysical Research*, 108 (C7), doi:10.1029/2000JC000441
- Carrère, L. and Lyard, F., 2003. Modeling the barotropic response of the global ocean to atmospheric wind and pressure forcing – comparisons with observations, *Geophysical Research Letters*, 30(6), 1275. doi:10.1029/2002GL016473
- Carrère, L.; Lyard, F.; Cancet, M.; Guillot, A., and Roblou, L., 2012. FES2012: A new global tidal model taking advantage of nearly twenty years of altimetry. *Proceedings of the 20 Years of Progress in Radar Altimetry Symposium* (Venice, Italy).
- Fok, H. S.; Baki Iz, H.; Shum, C. K.; Yuchan, Yi.; Andersen, O.; Braun, A.; Yi, Chao; Han, G.; Kuo, C. Y.; Matsumoto, K., and Song, T., 2010. Evaluation of Ocean Tide Models Used for Jason-2 Altimetry Corrections. *Marine Geodesy*, 33(S1), 285-303.
- Joseph, A.; Vijaykumar, K.; Mehra, P.; Unnikrishnan, A.S.; Sundar, D., and Desai, R.G.P., 2009. Observed tides at Mumbai High offshore region near the continental shelf break in the eastern Arabian Sea. *Current Science*, 96(9), 1233-1235.
- Kunte, P.D., 2008. Sediment concentration and bed form structures of Gulf of Cambay from remote sensing. *International Journal of Remote Sensing*, 29(8), 2169-2182.
- Le Bars, Y.; Lyard, F.; Jeandel, C., and Dardengo, L., 2010. The AMANDES tidal model for the Amazon estuary and shelf. *Ocean Modelling*, 31(3-4), 132-149.
- Le Provost C.; Genco, M.L.; Lyard, F.; Vincent, P., and Canceil, P., 1994. Tidal spectroscopy of the world ocean tides from a finite element hydrodynamic model. *Journal of Geophysical Research*, 99(C12), 24777-24798.
- Lyard, F.; Lefevre, F.; Letellier, T., and Francis, O., 2006. Modelling the global ocean tides: modern insights from FES2004. *Ocean Dynamics*, 56, 394-415.
- Lyard, F.; Roblou, L., and Birol, F., 2009. Precise error budget for the altimeter-derived tidal constants in shelf and coastal seas. *Ocean Surface Topography Science Team (OSTST)*, (Seattle, Washington).
- Lynch, D.R. and Gray, W. G., 1979. A wave equation model for finite element tidal computations, *Computers and Fluids*, 7, 207-228.
- Lewis, M.; Horsburgh, K., and Bates, P., 2014. Bay of Bengal cyclone extreme water level estimate uncertainty. *Natural Hazards*, 1-14. DOI 10.1007/s11069-014-1046-2.

- Maraldi C.; Galton-Fenzi, B.; Lyard, F.; Testut, L., and Coleman, R., 2007. Barotropic tides of the Southern Indian Ocean and the Amery Ice Shelf cavity. *Geophysical Research Letters*, 34(18), doi:10.1029/2007GL030900.
- Murty, T. S. and Henry, R.F., 1983. Tides in the Bay of Bengal. *Journal of Geophysical Research*, 88(C10), 6069–6076.
- Nayak, R. K. and Shetye, S.R., 2003. Tides in the Gulf of Khambhat, west coast of India. *Estuarine Coastal and Shelf Science*, 57, 249-254.
- Ray, R.; Egbert, G.D., and Erofeeva S.Y., 2011. Tide Predictions in Shelf and Coastal Waters : Status and Prospects. In: Vignudelli, S.; Kostianoy, A.G.; Cipollini, P., and Benveniste, J., (eds.), *Coastal Altimetry*. Berlin: Springer, pp. 191-216.
- Ray, R. D., 1999. A global ocean tide model from Topex/Poseidon altimetry: GOT99.2, *NASA Technical Memo, 209478*, Goddard Space Flight Center, Greenbelt, 58 pp.
- Sanil Kumar, V.; Dora, G.U.; Philip, C.S.; Pednekar, P.S., and Singh, P., 2011. Variations in tidal constituents along the nearshore waters of Karnataka, west coast of India. *Journal of Coastal Research*, 27(5), 824-829.
- Shum, C.K.; Woodworth, P.L.; Andersen, O.B.; Egbert, G.D.; Francis, O.; King, C. et al., 1997. Accuracy assessment of recent ocean tide models. *Journal of Geophysical Research*, 102(C11), 25173-25194.
- Sindhu, B.; Suresh, I.; Unnikrishnan, A.S.; Bhatkar, N.V.; Neetu, S., and Michael, G.S., 2007. Improved bathymetric datasets for the shallow water regions in the Indian Ocean, *Journal of Earth System Science*, 116(3), 261-274.
- Sindhu, B. and Unnikrishnan, A. S., 2013. Characteristics of Tides in the Bay of Bengal. *Marine Geodesy*, 36(4), 377-407.
- Smith, W. H. and Sandwell, D.T., 1997. Global sea floor topography from satellite altimetry and ship depth soundings. *Science*, 277(5334), 1956-1962.
- Saraceno, M. and Etcheverry, L.A.R., 2009. Tide model comparison in Patagonian Shelf. *3rd Coastal Altimetry Workshop, ESA-ESRIN*, (Frascati, Italy).
- Testut, L.; Birol, F, and Delebecque, C., 2012. Regional Tidal Modeling and Evaluation of Jason-2 Tidal Geophysical Correction, *Marine Geodesy*, 35(1), 299-313.
- Unnikrishnan, A.S.; Shetye, S.R., and Michael, G.S., 1999. Tidal propagation in the Gulf of Khambhat, Bombay High and surrounding areas. *Proceedings Indian Academy of Science (Earth Planet Science)*, 108(3), 155-177.
- Unnikrishnan, A.S., 2010. Tidal propagation off the central west coast of India. *Indian Journal of Geo-Marine Sciences*, 39(4), 485-488.
- Vignudelli, S.; Kostianoy, A.G.; Cipollini, P., and Benveniste, J., 2011. *Coastal Altimetry*. Berlin: Springer, 565p.

Figure 1: Map of the RMS misfits for M2 (cm), computed using Equation 2 between GOT4.7 and FES2012 Hydrodynamic tidal solutions. The green rectangle indicates the zone of interest of the present study, the West Indian coast.

Figure 2: The left panel shows depth contour of the inner shelf bathymetry (0-100 m). The black dot indicates the position of tide gauges used for validation. The two tracks (66 and 79) used as boundary conditions are shown. Right panel shows the model mesh along the west coast of India. The embedded upper right panel is a zoom of the mesh inside the Gulf of Khambhat. The spatial resolution of the mesh ranges from less than 1 km at the coast to a maximum of 20 km in the open ocean. Bathymetric features outside the model domain are also shown.

Figure 3: The bathymetry sensitivity test for M2 and K1. The test is represented as the RMS error (cm and log scale), as defined by Equation 2 in function of the station number (see Figure 2 and Table 1). The colored legend inside the plot box describes the tested parameter. The constituent RMS error (cm), as defined by Equation 4, is shown on the right side of the box with the corresponding parameter color. The parameter which gives the lowest RMS error is plotted with a thicker line.

Figure 4: The bottom friction sensitivity test for K1 (two upper boxes) and M2 (two lower boxes). The boxes on the left side correspond to a broad range of C_D values (from 0 to 7×10^{-3}) and the two on the right side to a narrow band of C_D values (roughly from 1×10^{-3} to 2×10^{-3}). Legend is the same as in Figure 3, except for the scale which is linear.

Figure 5: The open boundary sensitivity test for K1 and M2. Legend is the same as in Figure 3, except for the scale which is linear.

Figure 6: Comparison for the 39 validation sites ordered along the coast from South (station no.1) to North (station no.39) between the model (black) and the observation (grey). The two upper plots are for the phases (G) and phase differences (ΔG) in degrees and the two lower ones show amplitudes (A) and amplitude differences (ΔA) in cm. The right panels are the corresponding scatter plots for amplitude and phase respectively. All phases are referred to as Greenwich meridian Time, GMT.

Figure 7: Map of amplitude A (left panel) and phase G (right panel) of the M2 constituent of the model in the region of the Gulf of Khambhat. The contours indicate amplitude in meter on the left panel and

the phase in degree on the right panel. Location and name of the used tide gauge are shown in the left panel and their observed amplitude/phase in the right panel (in the same units as the contour lines).

Figure 8: Map of amplitude A (left panel) and phase G (right panel) of the S2 constituent of the model in the region of the Gulf of Khambhat. The contours indicate amplitude in meter on the left panel and the phase in degree on the right panel. Location and name of the used tide gauge are shown in the left panel and their observed amplitude/phase in the right panel (in the same units as the contour lines).

Figure 9: Map of amplitude A (left panel) and phase G (right panel) of the K1 constituent of the model in the region of the Gulf of Khambhat. The contours indicate amplitude in meter on the left panel and the phase in degree on the right panel. Location and name of the used tide gauge are shown in the left panel and their observed amplitude/phase in the right panel (in the same units as the contour lines).

Figure 10: Map of amplitude A (left panel) and phase G (right panel) of the O1 constituent of the model in the region of the Gulf of Khambhat. The contours indicate amplitude in meter on the left panel and the phase in degree on the right panel. Location and name of the used tide gauge are shown in the left panel and their observed amplitude/phase in the right panel (in the same units as the contour lines).

Table 1: Tidal misfits (cm), as defined in the text, between model and observation. Misfits are given for the 39 selected tidal gauges and the principal tidal constituents. The first row is the station number as indicated on Figure 6.

Table 2: Tidal RSS error (cm) for the full dataset (column 2), the 20 tide gauges located in the southern part of the domain (column 3) and the 19 remaining tide gauges located in the northern part of the domain (column 4) where the shelf is wide. The RSS are computed for the FES2004, FES2012, GOT4.7 and TPXO7.2 tidal atlases.

TABLE 1

N	TG	M2	S2	N2	K2	K1	O1	P1	Q1	M4	σ_{site}
1	Colachel	0.4	0.5	1.1	0.5	1.3	0.4	0.5	0.1	0.3	2.0
2	Vilinzam	0.7	2.3	1.1	0.1	0.3	0.6	0.5	0.1	0.4	2.8
3	Nindakara	2.0	3.3	1.4	0.4	2.7	1.8	0.7	0.8	0.4	5.3
4	Alleppey	1.5	1.4	0.8	0.6	1.2	1.3	1.3	0.5	--	3.2
5	Ponnani	3.2	1.7	1.2	0.4	0.9	1.4	3.6	0.4	--	5.6
6	Beyepore	3.3	1.1	0.7	1.0	1.2	1.4	0.8	0.4	0.3	4.3
7	Can0ore	1.0	1.3	2.6	0.4	3.9	1.0	1.4	0.3	0.2	5.3
8	Kasargod	2.8	1.9	1.0	0.3	0.8	1.3	0.6	0.3	0.2	3.9
9	Malpe	2.3	0.9	0.9	0.2	0.9	1.2	0.2	0.2	0.9	3.1
10	Coondapore	0.2	0.9	1.0	--	2.4	0.5	--	0.9	0.5	2.9
11	Honnavar	2.2	1.8	1.3	--	1.8	0.8	--	0.3	0.6	3.7
12	Kumta	4.9	2.5	1.9	0.8	0.5	0.7	1.2	0.5	0.4	6.1
13	Karwar	0.3	0.4	0.3	0.4	0.2	0.7	0.2	0.3	0.5	1.1
14	Marmagao	1.1	0.1	0.7	0.1	0.4	0.6	0.1	0.7	0.1	1.6
15	Vengurla	0.3	0.9	1.2	0.3	0.5	0.6	0.9	0.5	0.3	2.0
16	Malvan	0.8	1.1	1.0	0.7	1.2	0.6	1.0	0.5	0.4	2.5
17	Achra	4.2	2.2	1.9	0.9	0.9	1.5	0.9	0.5	1.1	5.6
18	Devgarh	0.7	1.1	0.8	0.9	0.8	0.1	1.0	0.1	0.3	2.2
19	Muskazi	1.0	0.8	0.7	0.5	2.2	0.8	1.7	0.4	0.4	3.3
20	Ratnagiri	0.2	0.4	0.2	0.2	1.1	0.7	0.8	0.4	0.6	1.7
21	Jaigarh	2.0	1.3	1.2	1.0	0.7	0.8	1.1	0.6	0.3	3.3
22	BoriaBay	1.3	1.4	1.9	1.0	0.8	0.5	1.0	0.2	0.4	3.2
23	Mumbai-high	2.5	2.5	2.3	--	3.2	0.9	--	--	--	5.4
24	Harnai	1.1	0.7	1.8	1.0	2.2	0.5	1.4	0.1	0.4	3.6
25	Shrivardhan	1.2	1.0	1.0	1.0	3.4	0.4	2.1	0.5	0.6	4.6
26	Janjira	2.3	1.3	1.9	1.1	5.6	1.1	2.8	1.0	1.4	7.4
27	Revadanda	7.5	3.4	2.2	1.9	4.8	0.3	2.6	0.4	1.5	10.4
28	RevasBandar	7.5	5.3	1.5	2.6	2.1	1.4	1.3	0.4	4.2	10.9
29	Bandra	5.9	3.7	0.9	1.4	2.2	0.5	1.3	0.4	1.4	7.7
30	Arnala	9.2	3.4	2.3	1.6	2.2	0.7	1.4	0.5	1.0	10.7
31	Kelve(Mahim)	9.7	3.1	2.0	1.9	3.9	0.4	1.9	1.3	1.1	11.5
32	Satpati	11.3	3.5	4.9	1.9	5.3	0.6	2.6	1.1	0.2	14.3
33	Umbargaon	16.5	3.2	5.0	2.0	9.4	3.6	3.6	2.2	3.7	21.1
34	Bulsar	23.1	7.0	7.5	2.6	18.1	2.6	7.2	2.1	3.8	32.4
35	Hazira(2nd)	35.7	7.8	7.3	3.3	20.1	7.5	7.0	2.8	2.1	43.9
36	PipavavBandar	20.6	2.6	--	--	5.6	1.3	--	--	--	21.6
37	Jafarabad	18.3	5.1	5.3	1.5	3.5	1.0	2.0	0.2	2.5	20.4
38	Nawabandar	6.9	2.1	2.6	0.9	2.5	1.2	1.9	1.0	0.9	8.5
39	Kotra	6.1	4.4	4.0	0.9	2.1	3.3	1.6	0.8	0.7	9.6
$\sigma_{\text{constituent}}$		9.5	2.9	2.6	1.2	5.2	1.7	2.2	0.9	1.4	RSS=12.0

TABLE2

MODEL	RSS Misfits (cm)		
	Full data set no.1-39	South no.1-20	North no.21-39
T-UGOm	12.0	3.7	16.8
GOT4.7	20.8	3.7	29.6
FES2012-HYDRO	21.0	4.8	29.7
TPXO7.2	23.1	4.0	32.8
FES2004	49.3	5.5	70.3

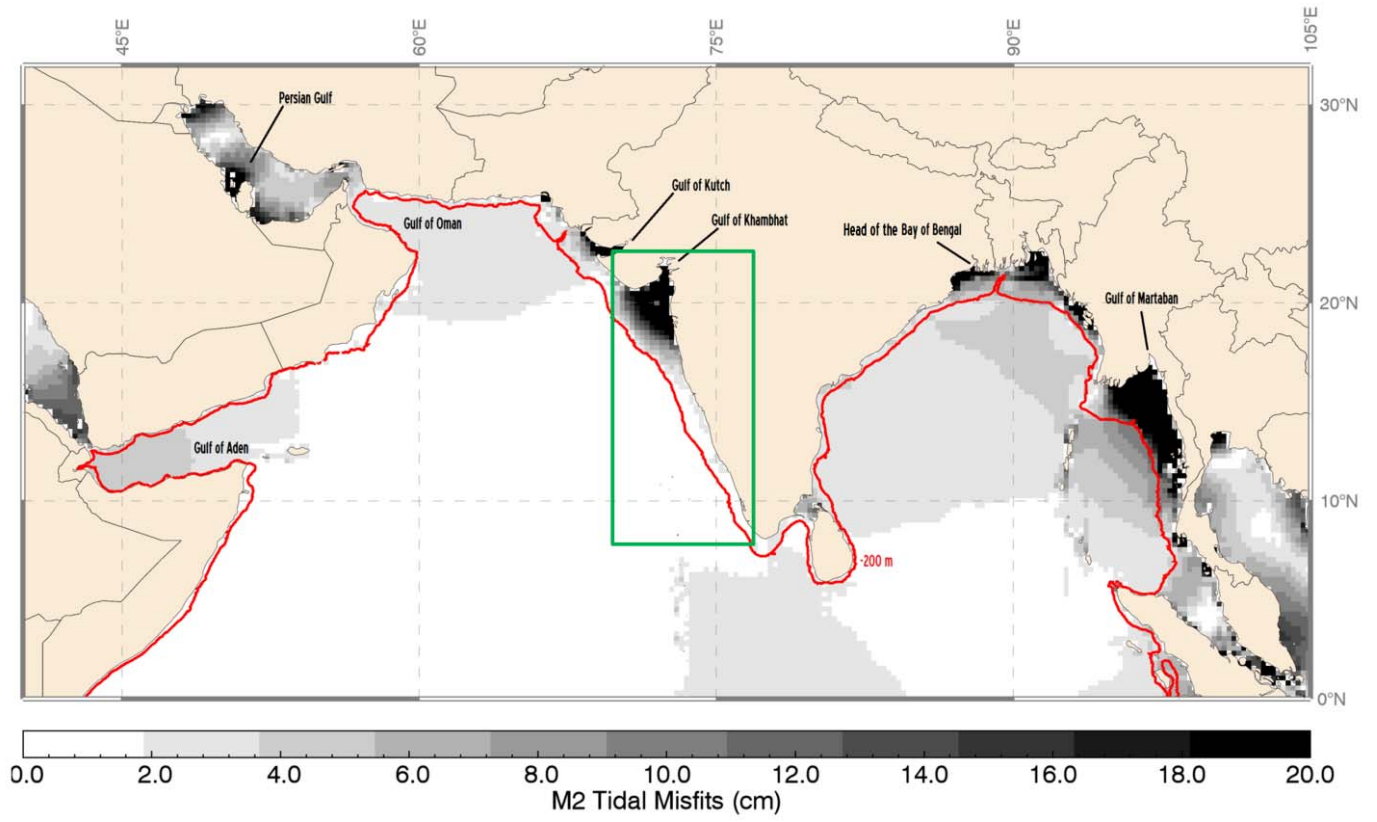


Fig. 1

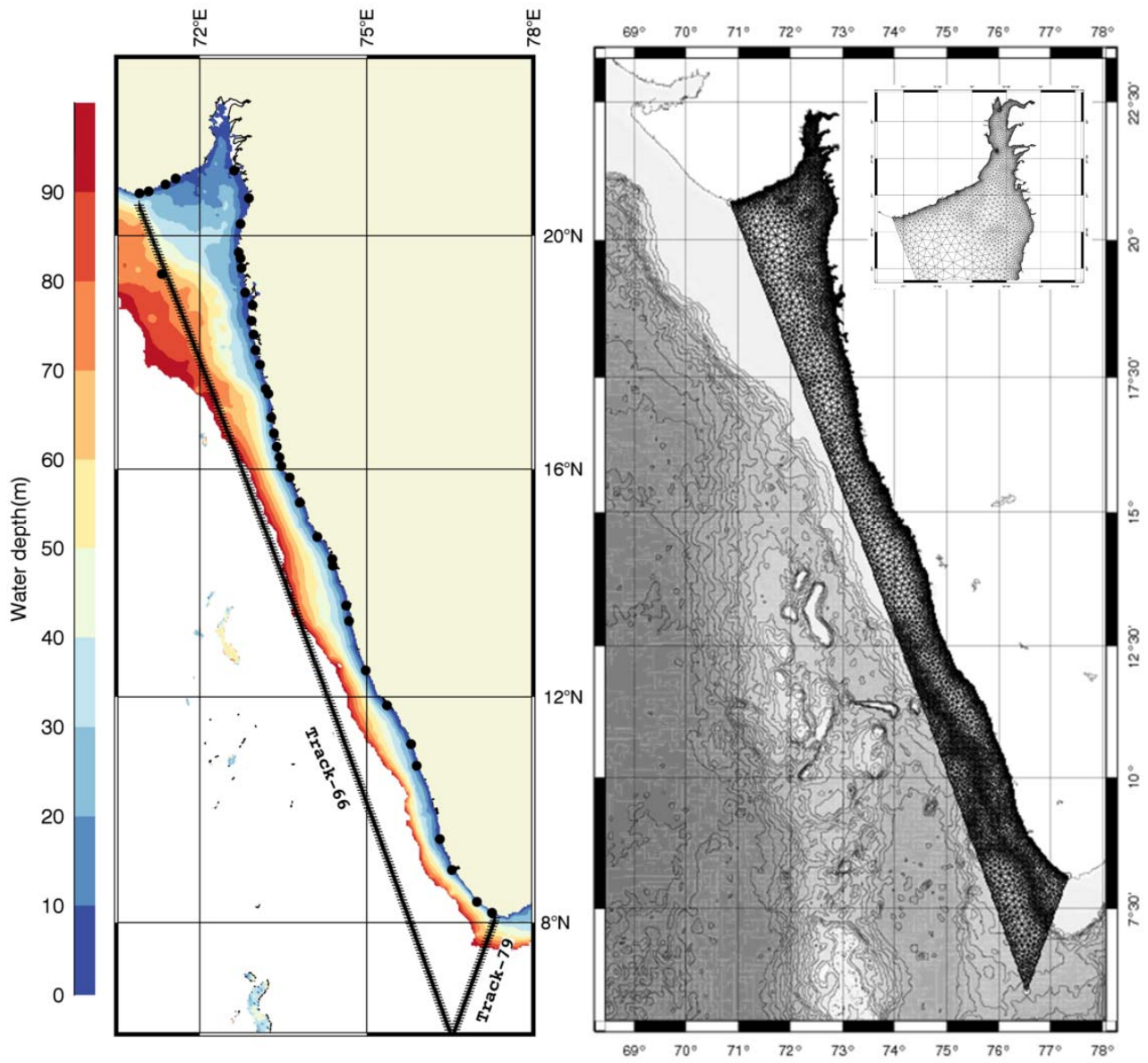


Fig. 2

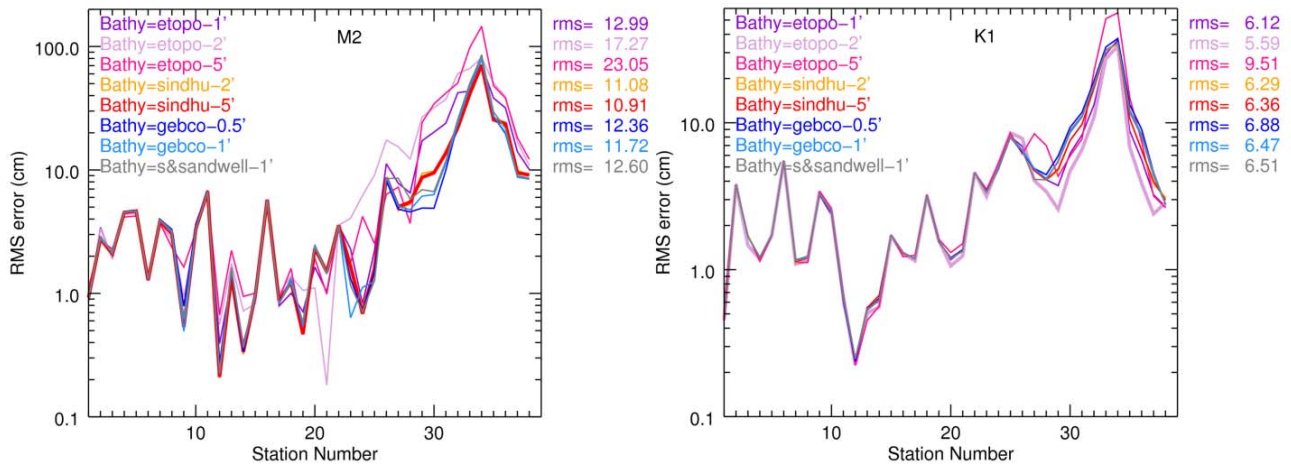


Fig.3

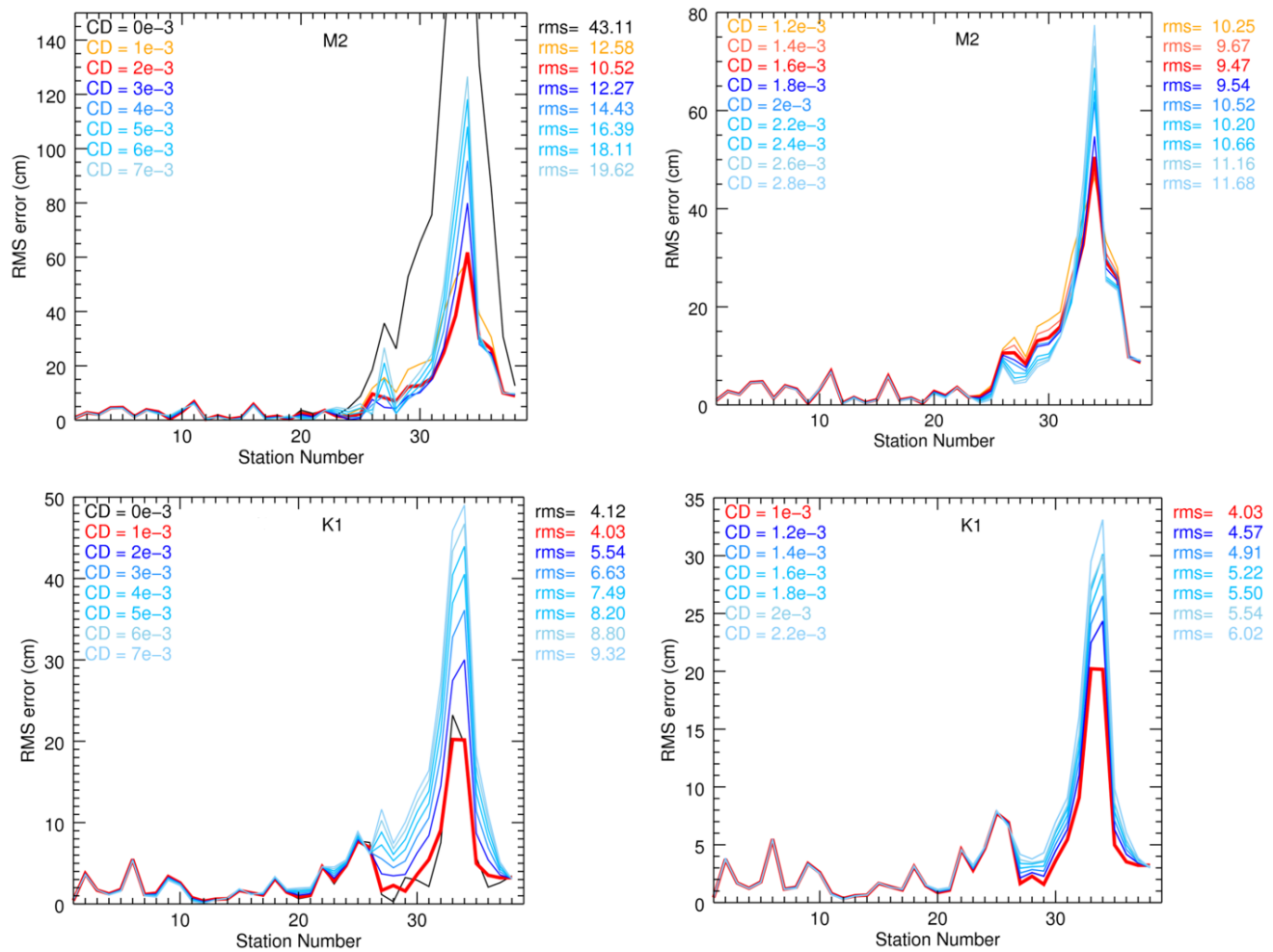


Fig. 4

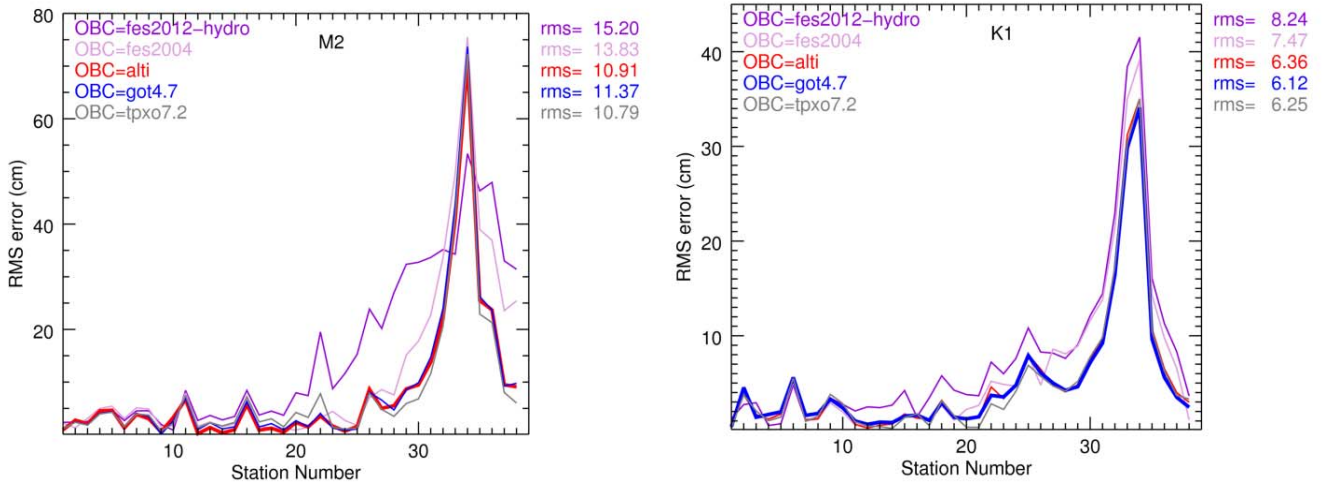


Fig. 5

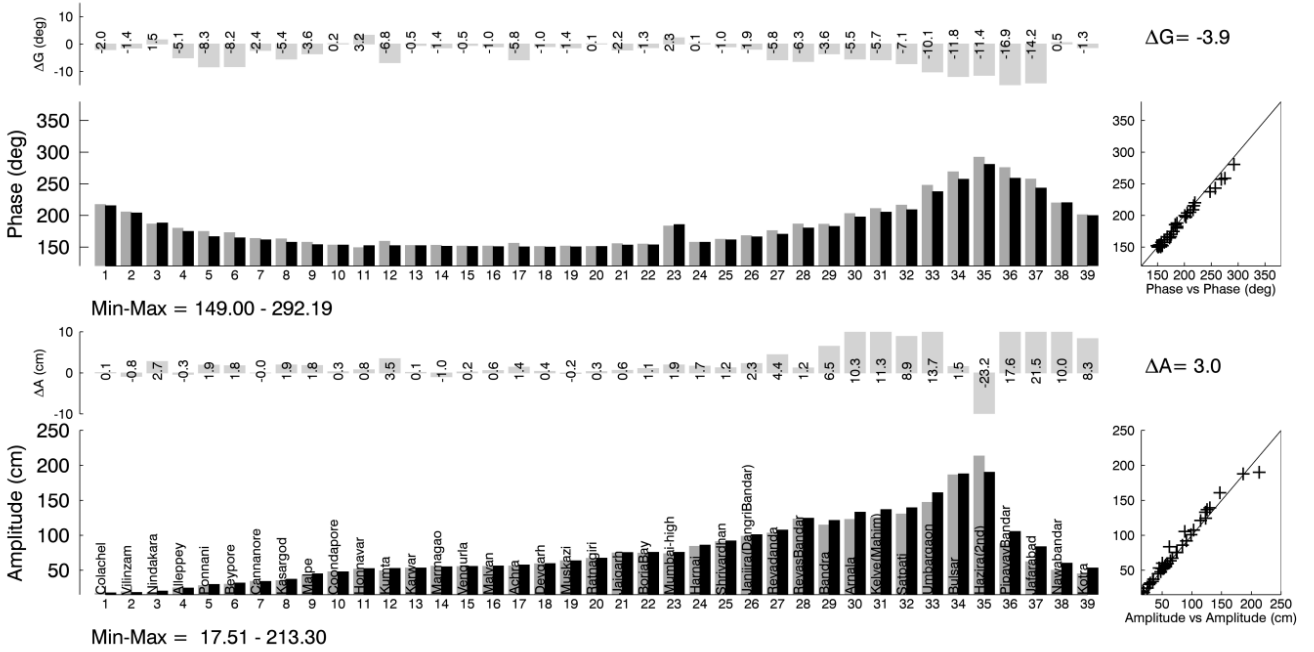


Fig. 6

AMPLITUDE

M2

PHASE

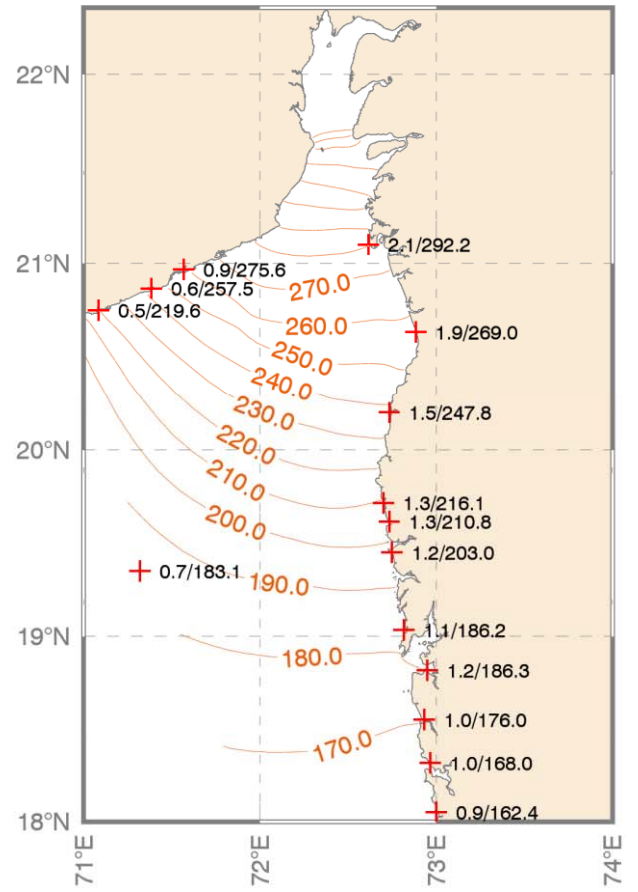
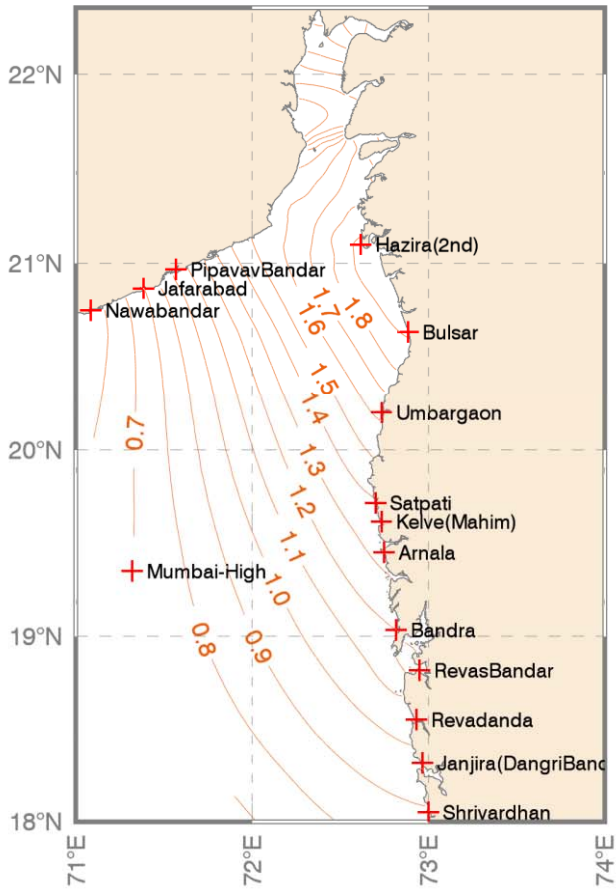


Fig. 7

S2

AMPLITUDE

PHASE

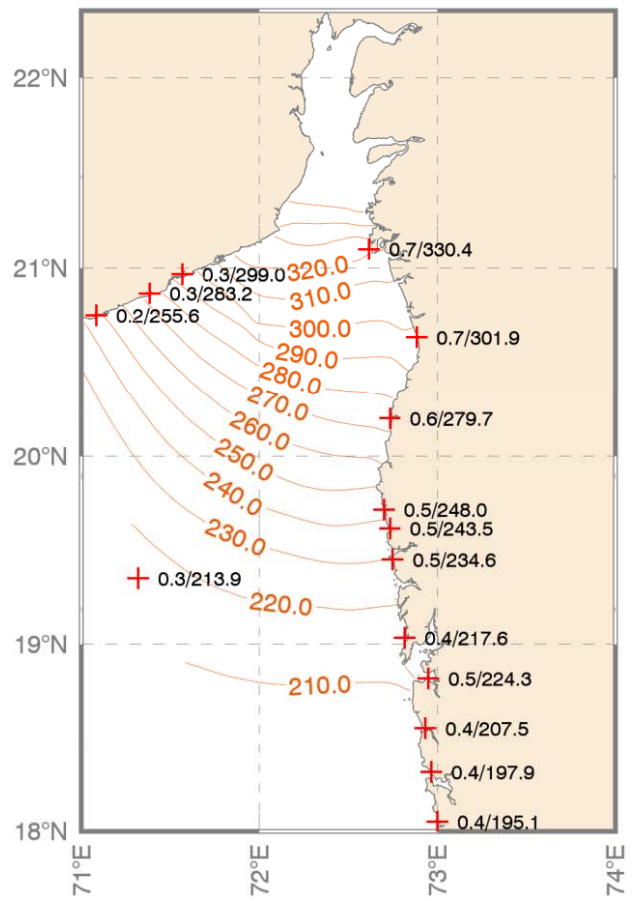
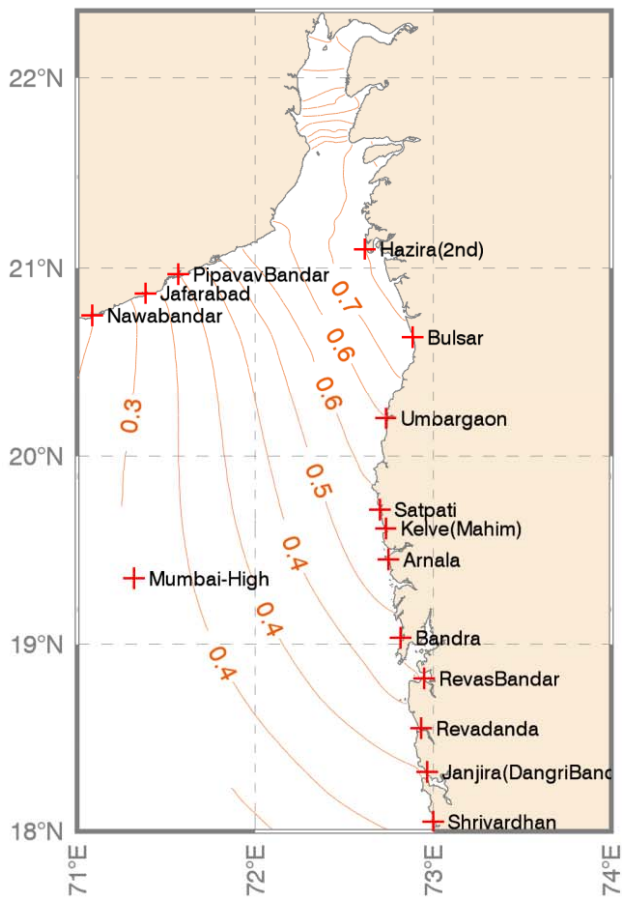


Fig. 8

AMPLITUDE

K1

PHASE

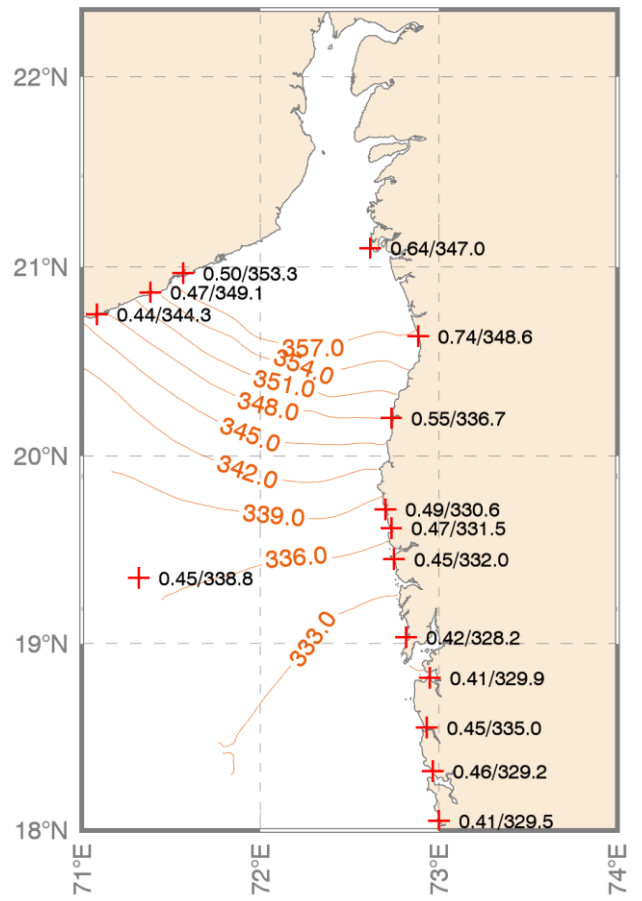
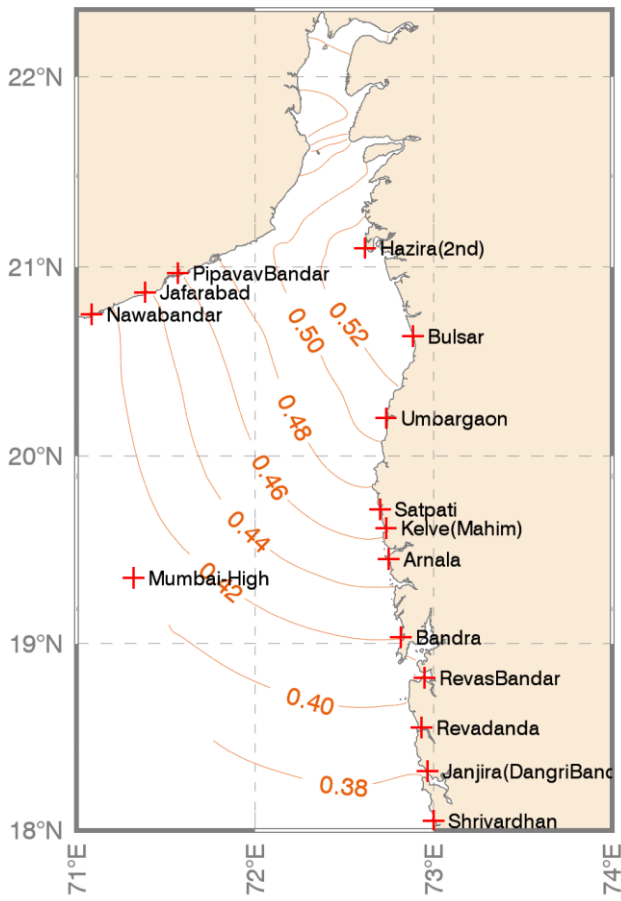


Fig. 9

AMPLITUDE

O1

PHASE

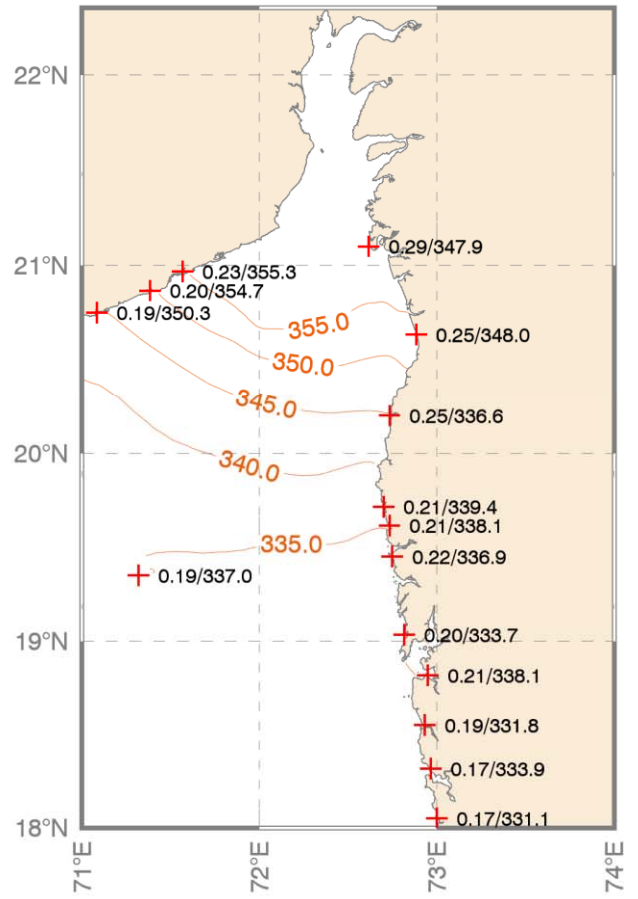
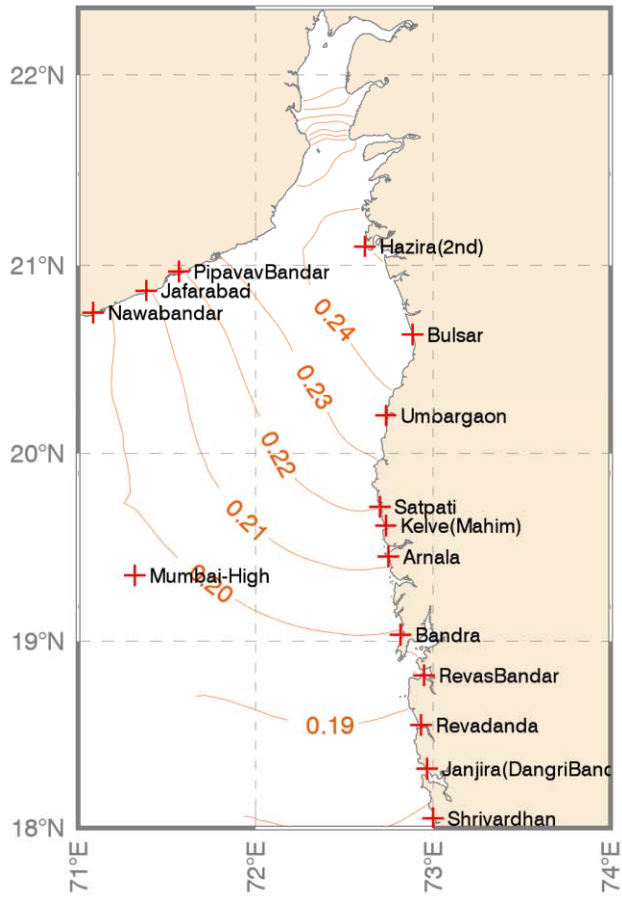


Fig. 10